New empirical formula for (γ, n) reaction cross section near GDR peak for elements with $Z \geqslant 60$

Rajnikant Makwana[1;1)] S. Mukherjee[1] Jian-Song Wang(王建松)[2] Zhi-Qiang Chen(陈志强)[2]

[1] Physics Department, Faulty of Science, The Maharaja Sayajirao University of Baroda, Vadodara-390002. India

[2] Key Laboratory of High Precision Nuclear Spectroscopy and Center for Nuclear Matter Science, Institute of Modern Physics, Chinese Academy of Science, Lanzhou 730000, China

Abstract: A new empirical formula has been developed that describes the (γ, n) nuclear reaction cross sections for isotopes with $Z \geqslant 60$. The results were supported by calculations using TALYS – 1.6 and EMPIRE – 3.2.2 nuclear modular codes. The energy region for incident photon energy has been selected near the giant dipole resonance (GDR) peak energy. The evaluated empirical data were compared with available data in the experimental data library EXFOR. The data produced using TALYS – 1.6 and EMPIRE – 3.2.2 are in good agreement with experimental data. We have tested and presented the reproducibility of the present new empirical formula. We observe the reproducibility of the new empirical formula near the GDR peak energy is in good agreement with the experimental data and shows a remarkable dependency on key nuclei properties: the neutron, proton and atomic number of the nuclei. The behavior of nuclei near the GDR peak energy and the dependency of the GDR peak on the isotopic nature are predicted. An effort has been made to explain the deformation of the GDR peak in (γ, n) nuclear reaction cross sections for some isotopes, which could not be reproduced with TALYS – 1.6 and EMPIRE – 3.2.2. The evaluated data have been presented for the isotopes ^{180}W, ^{183}W, ^{202}Pb, ^{203}Pb, ^{204}Pb, ^{205}Pb, ^{231}Pa, ^{232}U, ^{237}U and ^{239}Pu, for which there are no previous measurements.

Keywords: photonuclear reactions, GDR, empirical formula, TALYS, EMPIRE, cross section

PACS: 25.20.-x **DOI:** 10.1088/1674-1137/41/4/044105

1 Introduction

Nuclear reactions are of prime importance in the application of nuclear reactor technology. Nuclear reactors (fusion-fission) require a complete dataset of neutron and photon induced reactions. Photonuclear reactions are becoming more important for fusion reactors and accelerator driven sub-critical system (ADS), where high-energy photons will be generated and subsequently interact with the materials. The study of (γ, n) reactions are important for a variety of current and emerging fields, such as radiation shielding design, radiation transport, absorbed dose calculations for medical, physics, technology of fusion-fission reactors, nuclear transmutation, and waste management applications [1, 2]. In a fusion reactor, during the plasma shot, de-confined runaway electrons can interact with the first wall of the reactor and produce high energy photons [3]. These high energy photons can open reaction channels like (γ, n), (γ, p), (γ, 2n), (γ, 3n), etc. The most prominent reaction is (γ, n), as it has a lower threshold than multi-neutron emission, whereas for charged particle emission the Coulomb barrier needs to be considered. Exact information on the cross section for such nuclear reactions is needed to perform accurate nuclear transport calculations. Tungsten (W) and beryllium (Be) are selected as first wall materials for the International Thermonuclear Experimental Reactor (ITER) fusion reactor [4]. Among tungsten isotopes, only ^{182}W (26.5%), ^{184}W (30.64%) and ^{186}W (28.43%) have experimental cross section data for the (γ, n) reaction. The cross sections of the (γ, n) reaction for ^{180}W (0.12%) and ^{183}W (14.31%) are needed, along with all the remaining long-lived unstable isotopes, as they will interact with high-energy photons during the confined runaways and disruption phase [5]. Gamma induced nuclear reactions are also important for nuclear transmutation (e.g. ^{234}U(γ, n)^{233}U), which is useful for nuclear safety and incineration. The importance of the gamma incineration technique has been studied in the case of many isotopes for nuclear waste management [6–8].

In ADSs, the high energy proton beam will interact with high Z elements such as W, Pb-Bi, Th and U, which will produce neutrons through spallation reactions

Received 30 May 2016

1) E-mail: rajniipr@gmail.com

[9]. This spallation process will produce high energy photons, which will subsequently interact with the materials. It is necessary to have a complete nuclear dataset of photonuclear reactions for all isotopes of these elements. This can be done by experimental measurements. The experimental measurements of the nuclear reaction cross-section are one of the important methods to complete the nuclear dataset. However, there are always limitations in the experimental measurements due to non-availability of all the energies of incident particles, and preparation of the target, which may itself be unstable. For complete nuclear data for several isotopes, nuclear modular codes such as TALYS – 1.6 and EMPIRE – 3.2.2 are available. Using these codes, one can predict the cross sections for different nuclear reaction channels. These codes basically use some nuclear models, and on the bases of the nuclear reaction theory, evaluation of the nuclear reaction data is done. The theory involved in photonuclear reaction cross section evaluation is discussed in the next section of the paper. Apart from this, nuclear systematics and empirical formulae provide alternative methods for such isotopes, and can efficiently predict the nuclear properties. Many authors have used this theoretical approach. Several systematics and empirical studies have already been made for photonuclear reactions [10]. These empirical formulae reduce experimental efforts, as they are basically dependent on well-known nuclear properties. A new empirical formula has been developed and tested with nuclear modular codes and experimental data for $Z \geqslant 60$ in the present paper. With the help of the present empirical formula, one can predict the cross section datasets for those isotopes where there is a complete lack of experimental data.

2 Theory of photo neutron production

The interaction of high energy photons with target material can cause ejection of the nucleon/s, depending upon the energy of the incident photon. This reaction is considered a photonuclear reaction. Photons should have sufficient energy above the binding energy of the nucleus for nucleon emission. As the nuclear binding energies are above 6 MeV for most isotopes, photons should have such a threshold energy [11]. There are three basic mechanisms for photonuclear reactions: (a) giant dipole resonance (GDR), (b) quasi-deuteron (QD) and (c) intranuclear cascade [12]. A photon with energy below 30 MeV follows the GDR mechanism. In this process, the photon energy is transferred to the nucleus by the oscillating electrical field of the photon, which induces oscillations among nucleons inside the nucleus. Photo neutron production is more probable since proton ejection needs to overcome a large Coulomb barrier. For different isotopes at a particular energy, there is a peak of photo neutron production for the (γ, n) reaction. This is called the GDR peak energy. For isotopes above $Z = 60$, the peak energies are between 10-18 MeV. Above 30 MeV, the photo neutron production is mainly due to the QD effect [12]. In this mechanism, a photon interacts with the dipole moment of a pair of proton-neutrons in place of the nucleus as a whole [12]. Above 140 MeV, photo neutron production results from photo-pion production [12]. Further study of thermal fluctuation on GDR parameters is also of interest and studies are ongoing [13–16].

3 Present empirical formula and theoretical calculations

According to the semi-classical theory of the interaction of photons with nuclei, the shape of the fundamental resonance of the photo absorption cross section follows a Lorentz curve [12, 17].

$$\sigma(E)=\frac{\sigma_i}{1+\left[\frac{\left(E_\gamma^2-E_{\mathrm{m}}^2\right)^2}{E_\gamma^2\gamma^2}\right]}, \tag{1}$$

where, σ_i, E_γ and γ are the Lorentz parameters: peak cross section, resonance energy and full width at half maximum respectively [18].

In a more general way, by using nuclear modular codes, such as TALYS – 1.6 and EMPIRE – 3.2.2, the photo absorption cross section is calculated as the sum of two components [19],

$$\sigma_{\mathrm{abs}}\left(E_\gamma\right)=\sigma_{\mathrm{GDR}}\left(E_\gamma\right)+\sigma_{\mathrm{QD}}\left(E_\gamma\right). \tag{2}$$

The component $\sigma_{\mathrm{GDR}}(E_\gamma)$ represents the GDR and is given by a Lorentzian shape, which describes the giant dipole resonance. It is given from Eq. (1) by the following expression:

$$\sigma(E)=\sum_i \frac{\sigma_i\cdot\left(E_\gamma\cdot\Gamma_i\right)^2}{\left(E_\gamma^2-E_i^2\right)^2+\left(E_\gamma\cdot\Gamma_i\right)^2}, \tag{3}$$

where σ_i, E_i and Γ_i are: peak cross section, resonance energy and full width at half maximum respectively. The summation is limited to $i=1$ for spherical nuclei, while for deformed nuclei the resonance is split and one uses $i=1,2$. The component $\sigma_{\mathrm{QD}}(E_\gamma)$, is given by Levinger type theory given by Chadwick et al [19–21]. It is basically from the quasi-deuteron model. In the energy range from the photonuclear threshold to 30 MeV, the GDR mechanism is dominant, and from 30 – 140 MeV the QD mechanism is dominant. Above 140 MeV the threshold energy for pion production is achieved [20].

The above theory has been used in the TALYS – 1.6 and EMPIRE – 3.2.2 nuclear modular codes [22, 23]. Further details of these codes are given in Refs. [18, 24]. Using these codes, (γ, n) nuclear reaction cross sections for different isotopes ($Z \geqslant 60$) were calculated and are presented in the present work. Until now, the photonuclear reaction cross sections have been evaluated using the Lorentz parameters. These parameters for several isotopes are calculated by fitting the experimental data or by systematics [25].

3.1 Fundamental term

In the present paper, in contrast to the Lorentzian parameters, the basic properties of nuclei, A, N and Z, are used to estimate the photonuclear cross section. Levovskii has given empirical formulas for (n, p) and (n, 2n) reaction cross section at 14.0 MeV [26] as,

$$\sigma(\mathrm{n,p}) \propto \sigma_{\mathrm{p}} \cdot \mathrm{e}^{-\frac{33\cdot(N-Z)}{A}}, \tag{4}$$

$$\sigma(\mathrm{n,2n}) \propto \sigma_{\alpha} \cdot \mathrm{e}^{-\frac{33\cdot(N-Z)}{A}}, \tag{5}$$

where $\sigma_{\mathrm{p}} = \pi r_0^2 (A^{1/3}+1)^2$ and $\sigma_{\alpha} = 0.4 \cdot \pi r_0^2 (A^{1/3}+1)^2$, $r_0 = 1.2 \times 10^{-13}$ cm.

These empirical formulae are based on A, N and Z of a nucleus, and at an energy 14.0 MeV. Similarly it is possible to derive an empirical formula for photo induced (γ, n) nuclear reactions, which may be applied near GDR peak energy. For the (γ, n) reaction, the formula is modified in the following way,

$$\sigma(\gamma,\ \mathrm{n}) \propto \sigma_{\mathrm{m}} \cdot \mathrm{e}^{-\frac{33.5\cdot(N-Z)}{A}}, \tag{6}$$

$$\sigma_{\mathrm{m}} = \pi r_0^2 \cdot (A^{2/3}+1)^2 \cdot (N-Z) \cdot A^{\frac{-4}{3}}, \tag{7}$$

where r_0 is the average nuclear radius.

3.2 Isotopic dependent resonance term

The term $(N-Z)/A$ is the asymmetry parameter which considers the deformation of a nucleus. In this expression, there is no term containing energy dependency. Hence, an energy dependent term must be added, and the modified formula is as given below,

$$\sigma(\gamma,\mathrm{n}) \propto \sigma_{\mathrm{m}} \cdot \mathrm{e}^{-\frac{33.5\cdot(N-Z)}{A}} \cdot \mathrm{e}^{\left(-\left(\frac{(E_i - S_j \cdot R_{\mathrm{p}})}{2}\right)^2\right)} \tag{8}$$

where E_i is the incident photon energy, and R_{p} is the resonance parameter.

The parameter S_j is given by,

$$S_j = \frac{A^2}{2\,(N-Z)^2}. \tag{9}$$

The parameter R_{p} is estimated for an isotope by fitting the (γ, n) nuclear reaction cross section using the above formula for different isotopes of the same element. We observed that this parameter R_{p} follows a linear relationship against the atomic mass of different isotopes of the same element, which can be written in the form of the following equation,

$$R_{\mathrm{p}} = m \cdot A + C, \tag{10}$$

where A is the atomic mass of the isotope, and m and C are slope and intercept respectively, More details of this parameter (R_{p}) for different elements is given in Section 3.3.1.

This term $\mathrm{e}^{-\left\{\frac{\left(E_i - S_j \cdot R_{\mathrm{p}}\right)}{2}\right\}^2}$ depends on the energy of the incident photon and the isotopic nature of the target nucleus. When a photon is incident on the nucleus the response of the nucleus depends on the photon energy. While the incident photon is below the threshold energy for photo, fission, the photon cannot eject a nucleon from the nucleus. If energy of the photon is above the threshold energy of the (γ, n) reaction, the reaction cross section increases until the resonance peak energy. After this energy, the cross section decreases again. This is incorporated using this exponential term. The subtraction of $S_j \cdot R_{\mathrm{p}}$ from the incident photon energy shows the isotopic dependence of the resonance peak energy of the reaction. As the isotopic number increases it is observed in the experimental data that the GDR peak shifts towards the lower energy side. This back shift effect can be calculated with the exponential term considered here. The value of $S_j \cdot R_{\mathrm{p}}$ increases with addition of neutrons to the isotope nucleus. This means that when a photon is incident on the target isotope, it interacts with the last shell neutron in the nucleus. The binding energy of the last added neutron will be least. Hence the photon may require smaller energy to cause the resonance as the isotope number increases.

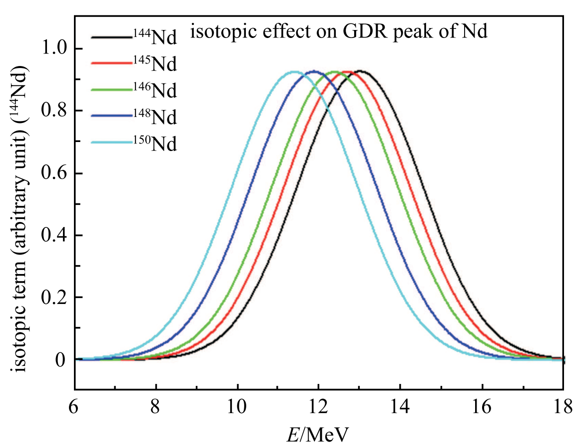

Fig. 1. (color online) Back shift of resonance peak energy in Nd isotopes, from the term $\mathrm{e}^{-\left\{\frac{\left(E_i - S_j \cdot R_{\mathrm{p}}\right)}{2}\right\}^2}$.

This can be observed from Figs. 1 and 2, showing the isotopic effect for the resonance peak energy back shift in Nd and Pt isotopes from the above exponential term.

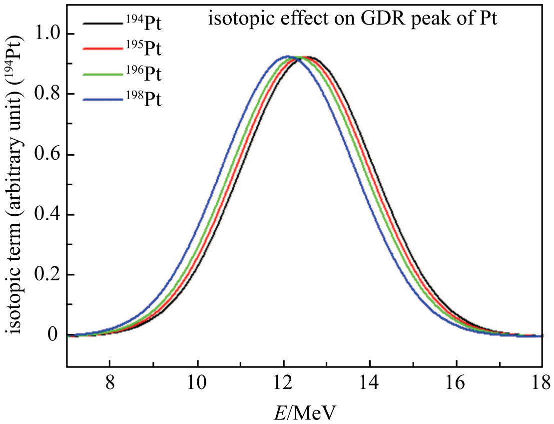

Fig. 2. (color online) Backshift of resonance Peak Energy in Pt isotopes, from the term $e^{-\left\{\frac{(E_i - S_j \cdot R_\mathrm{p})}{2}\right\}^2}$.

3.3 Energy dependency term

It was found that another energy related term is required to make the formula more efficient to predict the cross section. If the photon energy increases, then the photon can transfer more energy to the nucleus. In the GDR mechanism, the oscillating electrical field transfers its energy to the nucleus by inducing an oscillation in the nucleus, which leads to relative displacement of tightly bound neutrons and protons inside the nucleus [12].

When the energy of the photon is low (near threshold), the oscillating electric field of the photon interacts with the collective nucleus field produced by the sum effect of the nucleons. But as the energy of the photon increases, the oscillating electrical field interacts with a pair of neutron and proton rather than with the nucleus. This is followed by the term $e^{\sqrt{1+E^{\frac{2}{3}}}}$, where E is the energy of the incident photon. This term shows that the photon can have more energy to transfer to the nucleon as the incident photon energy increases. This indicates that as the energy of the photon increases, it can have less interaction time with nucleons, and hence the pre-equilibrium or direct reaction mechanism can be followed by the emission of the neutron.

Hence, by the addition of an energy dependent term, the modified formula is,

$$\sigma(\gamma,\mathrm{n}) \propto \sigma_\mathrm{m} \cdot e^{-\frac{33.5\cdot(N-Z)}{A}} \cdot e^{\left(-\left(\frac{(E_i - S_j \cdot R_\mathrm{p})}{2}\right)^2\right)} \cdot e^{\sqrt{1+E^{\frac{2}{3}}}}. \tag{11}$$

An additional factor S_f, which is an isospin dependent factor, has been introduced to complete the formula. This factor was plotted for different isotopes of the same element, and fitted. We observed this factor follows some exponential relation, which is described in Section 3.3.2.

This empirical formula gives the cross section to the order of milli-barns.

The final modified formula is now,

$$\sigma(\gamma,\mathrm{n}) = \sigma_\mathrm{m} \cdot e^{-\frac{33.5\cdot(N-Z)}{A}} \cdot e^{\left(-\left(\frac{(E_i - S_j \cdot R_\mathrm{p})}{2}\right)^2\right)} \cdot e^{\sqrt{1+E^{\frac{2}{3}}}} \cdot S_\mathrm{f}. \tag{12}$$

3.3.1 R_p parameter

This parameter shows the dependency of the photo absorption cross section with respect to the atomic number (Z). In the empirical formula, the term $e^{-\left\{\frac{(E_i - S_j \cdot R_\mathrm{p})}{2}\right\}^2}$ has a subtraction factor containing S_j and R_p. R_p is responsible for the change in the cross section due to atomic number, and the multiplication of S_j and R_p is responsible for the isotopic back shift effect, as shown in Figs. 1 and 2. The parameter R_p for different isotopes can be calculated using a linear relation, viz Eq. (10), with the atomic mass number of isotopes for an element. Therefore, the plot of R_p vs A for different elements should show parallel lines with different intercepts on the R_p axis, as shown in Fig. 3. Parallel lines have the same slope but different intercepts. Hence, the mean slope of different elements has been taken as the standard slope for all elements ($Z \geqslant 60$). This value of the slope (m) mentioned in Eq. (10) is $\sim$ 0.03164 $\pm$ 0.00409. The intercept C for different elements are plotted against the atomic number of the element, and fitted with the mathematical software MATLAB using a 3rd degree polynomial as shown in Fig. 4. The intercept C for different elements can be determined from the following equation:

$$C(Z) = p_1 \cdot Z^3 + p_2 \cdot Z^2 + p_3 \cdot Z + p_4 \tag{13}$$

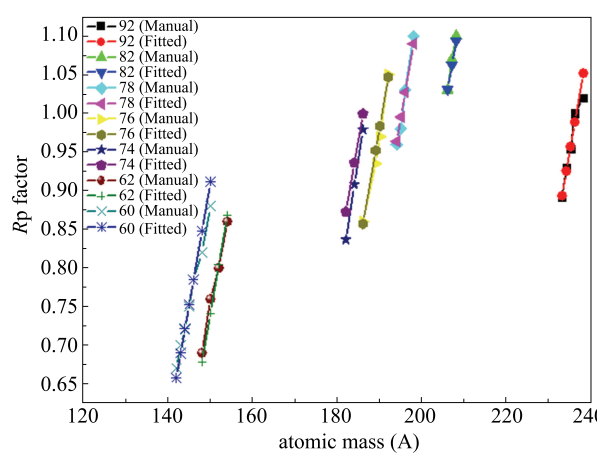

Fig. 3. (color online) R_p parameter fitting for different elements with Eq. (10).

with $p_1 = -4.155 \times 10^{-5}$, $p_2 = 0.008971$, $p_3 = -0.7156$, and $p_4 = 15.78$, where Z is atomic number (SSE: 0.00147;

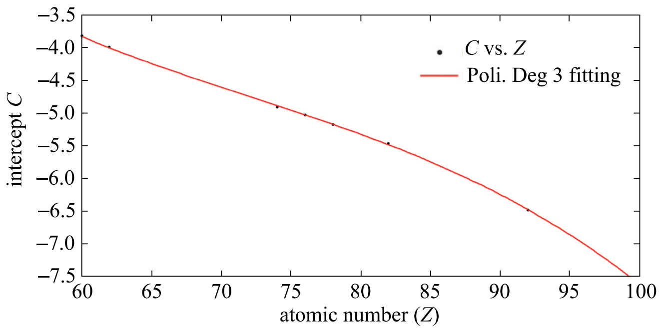

Fig. 4. Intercept C for Eq. (10) for different elements fitted with Eq. (11).

R-square: 0.9998: Adjusted R-square: 0.9996; RMSE: 0.01917).

Hence, the intercept for any element can be evaluated using the above Eq. (13). Using this intercept and the slope 0.03164 ± 0.00409, one can calculate the parameter $R_{\rm p}$ from Eq. (10). The model values of the parameter $R_{\rm p}$ for different elements are compared with the previous manually selected values in Fig. 3.

3.3.2 $S_{\rm f}$ parameter

This parameter includes the isospin effect. This effect has been discussed by J. S. Wang et al [27]. In order to include this effect in the empirical formula, an additional factor called $S_{\rm f}$ has been added. This factor was initially manually added and then, in order to generalize, it was fitted with different combinations of N, Z and A. It was found that it follows a complex exponential relation with $\exp((N{-}Z)/N)$ of an isotope. This parameter $S_{\rm f}$ is also considered a result of the asymmetry of the nucleus. As there is a difference in neutron and proton number, the fraction $(N-Z)/N$ is the available neutron fraction for a photon to eject. As this fraction value increases, the value of $S_{\rm f}$ increases correspondingly, which directly shows an increase in the photo absorption cross section of that isotope.

This isotopic factor $S_{\rm f}$ for different isotopes is plotted with respect to $\mathrm{e}^{\frac{N-Z}{N}}$ and fitted with MATLAB software as shown in Fig. 4. The generalized expression to determine the $S_{\rm f}$ parameter for an isotope is as given below:

$$S_{\rm f} = a\mathrm{e}^{bx} + c\mathrm{e}^{dx}, \tag{14}$$

where, $x = (N-Z)/N, a = 1.21 \times 10^{-22}$, $b = 34.21, c = 7.71 \times 10^{-11}$, $d = 14.52$ (SSE: 0.006977; R-square: 0.9781; Adjusted R-square: 0.9759; RMSE: 0.01551).

Looking at Fig. 5 carefully, for some points when $\mathrm{e}^{\frac{(N-Z)}{N}}$ is near 1.40 to 1.42, they have almost the same $S_{\rm f}$ factor values. These $S_{\rm f}$ factor values are for $Z = 82$ and $N = 124$, 125, 126, which are either a magic number or near the magic number. $S_{\rm f}$ is purely dependent on $(N-Z)/N$, which is a shell dependent term. The anomalous behavior of the same $S_{\rm f}$ factor values for these isotopes is because of the magic shell effect.

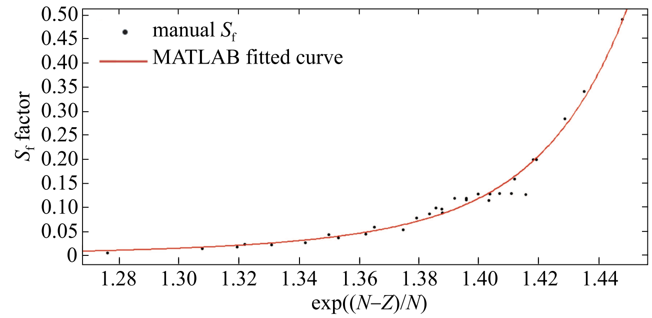

Fig. 5. $S_{\rm f}$ parameter for different $(N-Z)/N$ fitted with Eq. (14).

4 Results and discussion

The (γ, n) reaction cross sections are calculated using TALYS – 1.6, EMPIRE – 3.2.2 and the newly developed empirical formula for isotopes with $Z \geqslant 60$ and presented in Figs. 6–10. The cross sections are calculated for the energy range in which the GDR peak is observed. The theoretically calculated cross sections are compared with the experimentally available data in the EXFOR data library [28]. The data calculated using modular codes and empirical formula are in agreement with the experimental data, as shown in Figs.6–10. However, the cross section values and the nuclear behavior near the GDR peak predicted by the empirical formula are more appropriate. This empirical formula is good for those isotopes which have a single GDR peak. In most of the cases studied here that have a single GDR peak, the empirical formula gives good agreement near the GDR peak energy compared to the model based on Lorentz curve fitting.

In the case of isotopes with Z from 63 to 75, it is found that according to the collective model these isotopes have large nuclear quadrupole moments. The quadrupole exists because of the asymmetry of the nucleus. The nuclei are found in the middle of the 1d, 2 s shells in the range $145 < A < 185$. The energy difference between the ground state and the first excited state is of the order of hundreds of keV. In the deformed nucleus the incident photon can interact either with the ground state or with the excited state nucleon, and hence can produce a resonance at two different nearby energies. This is observed in the above isotopes. For such cases, the Lorentz curve based model, viz. TALYS – 1.6 and EMPIRE – 3.2.2, works reliably for these isotopes, as shown in Fig. 11. For some cases, however, the TALYS – 1.6 and EMPIRE – 3.2.2 model does not work well, e.g. Figs. 11(e – f). To apply the empirical formula for such isotopes, it is assumed that there may be two peaks due to unresolved resonances occurring near the energies of ground and excited nuclei, which are due to the quadrupole moment. This suggests parameters R_{p} and S_{f} can have two different values for these isotopes. It indicates that the energy dependence cross section curve is made of two curves with two different R_{p} (R_{p1} and R_{p2}) and S_{f} values (S_{f1} and S_{f2}) of parameters R_{p} and S_{f} respectively. These values can be estimated by multiplying the following factors to the R_{p} and S_{f} values calculated from Sections 3.3.1 and 3.3.2.

$$R_{\mathrm{p1}} = 0.95 \times R_{\mathrm{p}}, \tag{15}$$

$$R_{\mathrm{p2}} = 1.20 \times R_{\mathrm{p1}}, \tag{16}$$

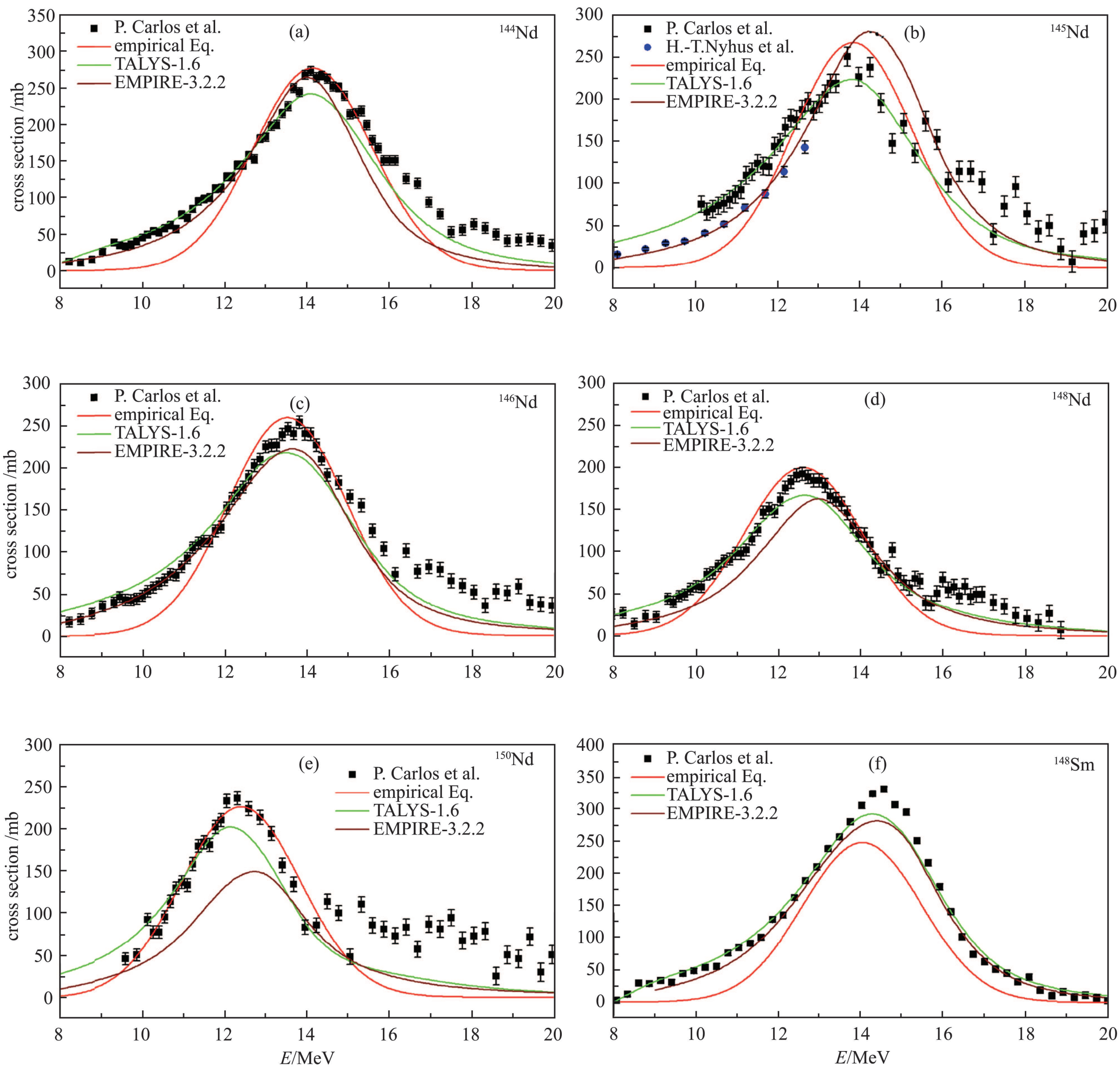

Fig. 6. (color online) Comparison of evaluated data using TALYS-1.6, EMPIRE-3.2.2, and empirical formula with experimental data from EXFOR, for ^{144}Nd, ^{145}Nd, ^{146}Nd, ^{148}Nd, ^{150}Nd, and ^{148}Sm.

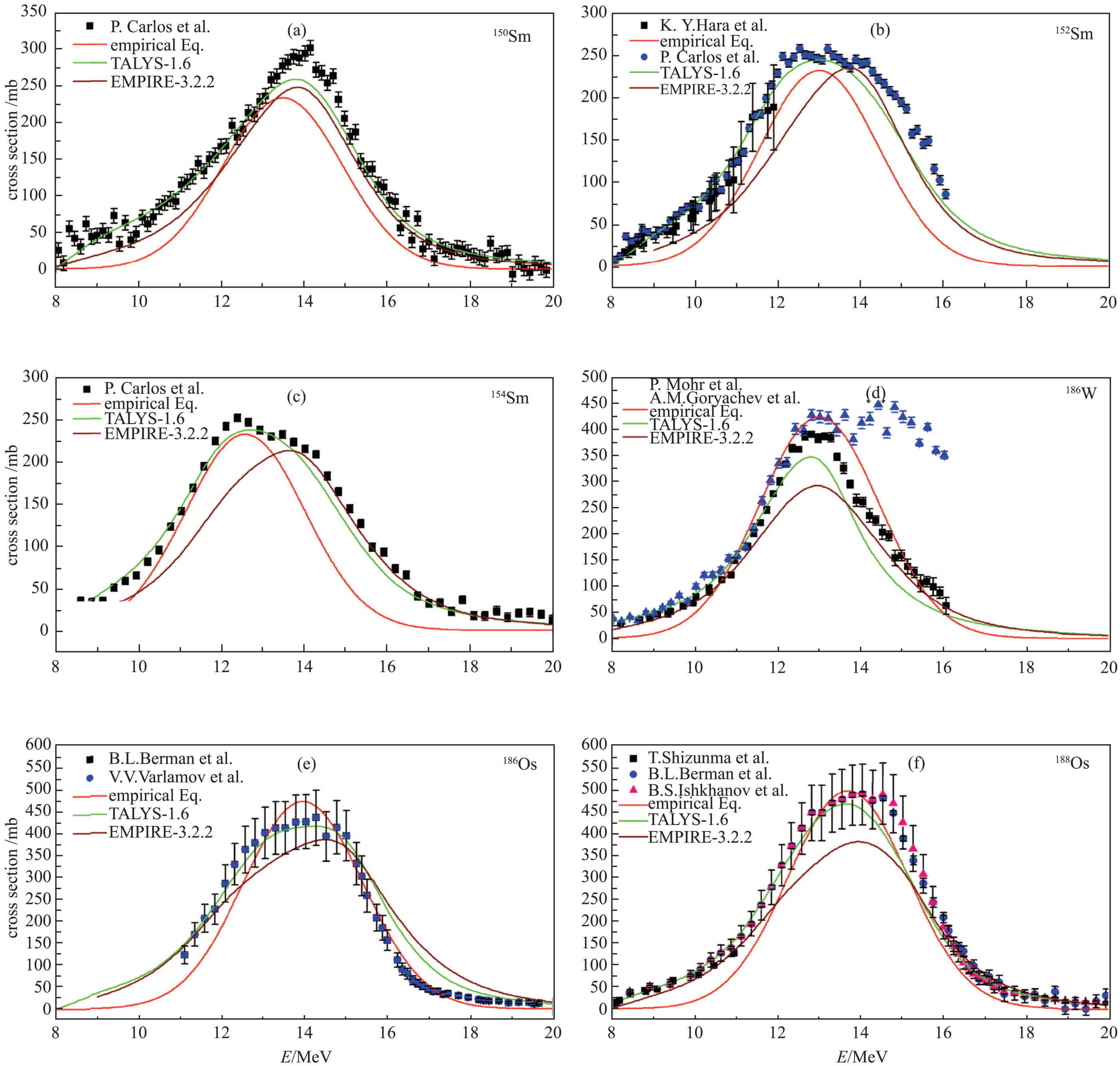

Fig. 7. (color online) Comparison of evaluated data using TALYS-1.6, EMPIRE-3.2.2, and empirical formula with experimental data from EXFOR, for ^{150}Sm, ^{152}Sm,^{154}Sm, ^{186}W, ^{186}Os, and ^{188}Os.

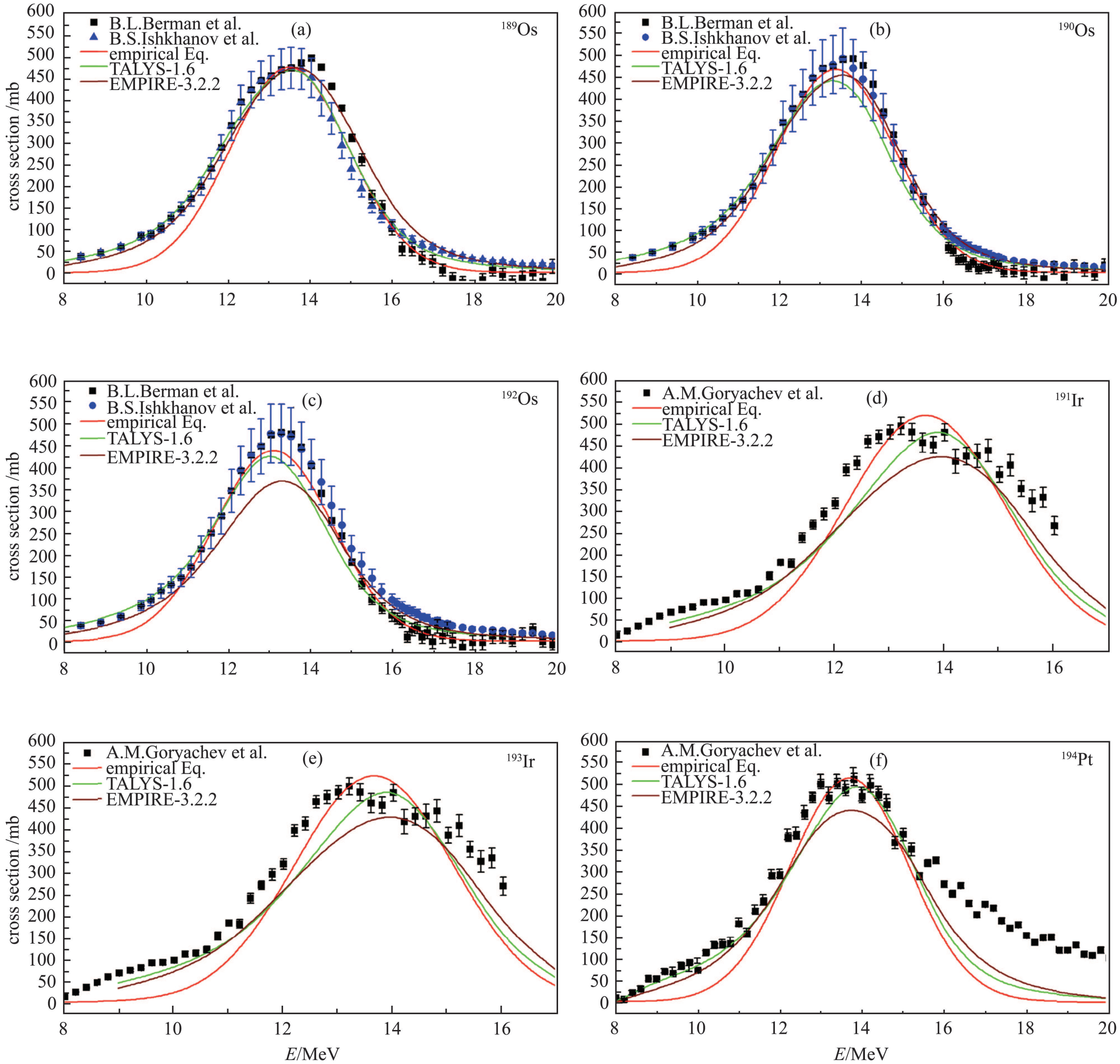

Fig. 8. (color online) Comparison of evaluated data using TALYS-1.6, EMPIRE-3.2.2, and empirical formula with experimental data from EXFOR, for ^{189}Os, ^{190}Os, ^{192}Os, ^{191}Ir, ^{193}Ir, and ^{194}Pt.

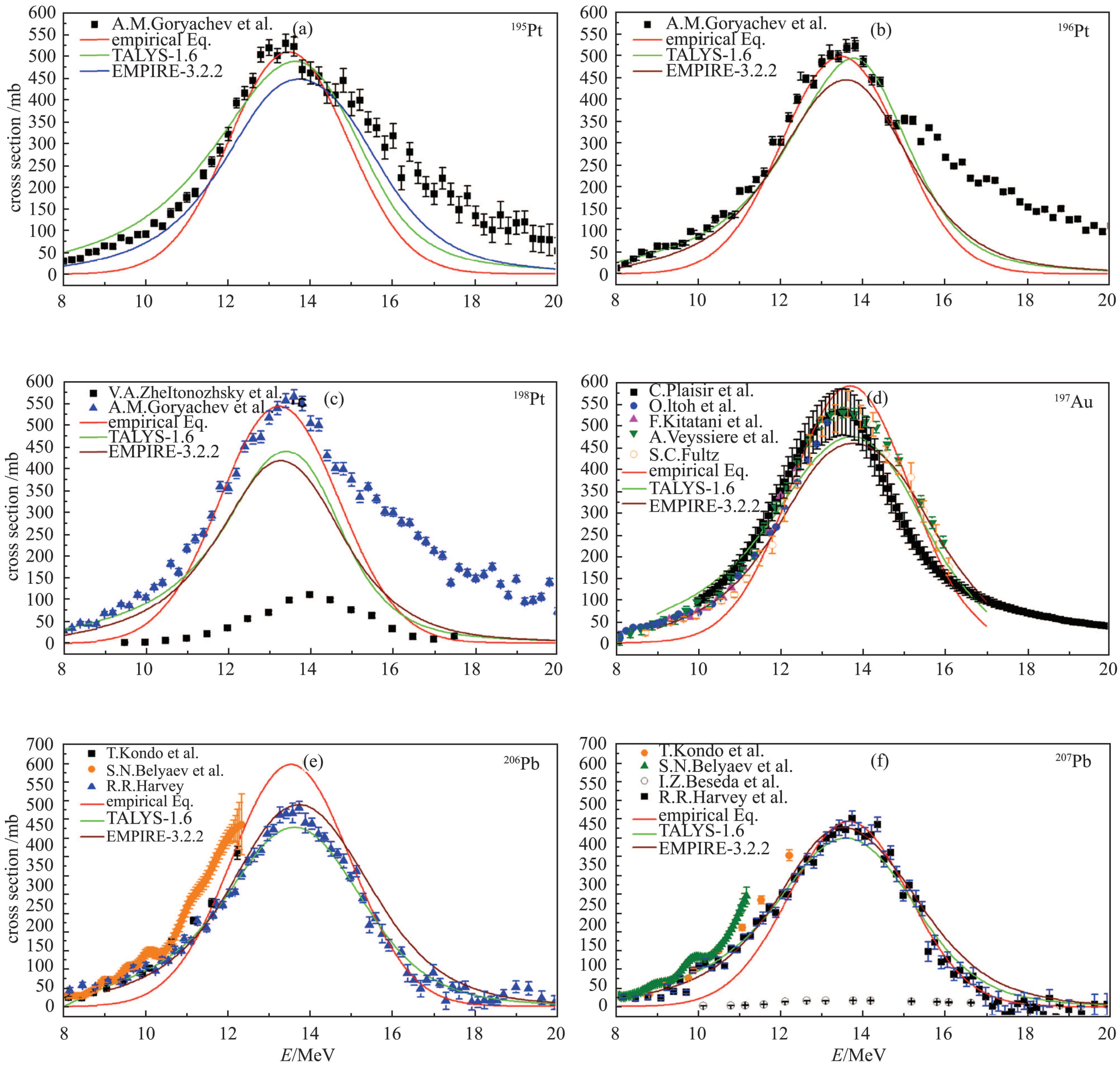

Fig. 9. (color online) Comparison of evaluated data using TALYS-1.6, EMPIRE-3.2.2, and empirical formula with experimental data from EXFOR, for ^{195}Pt, ^{196}Pt, ^{198}Pt, ^{197}Au, ^{206}Pb, and ^{207}Pb.

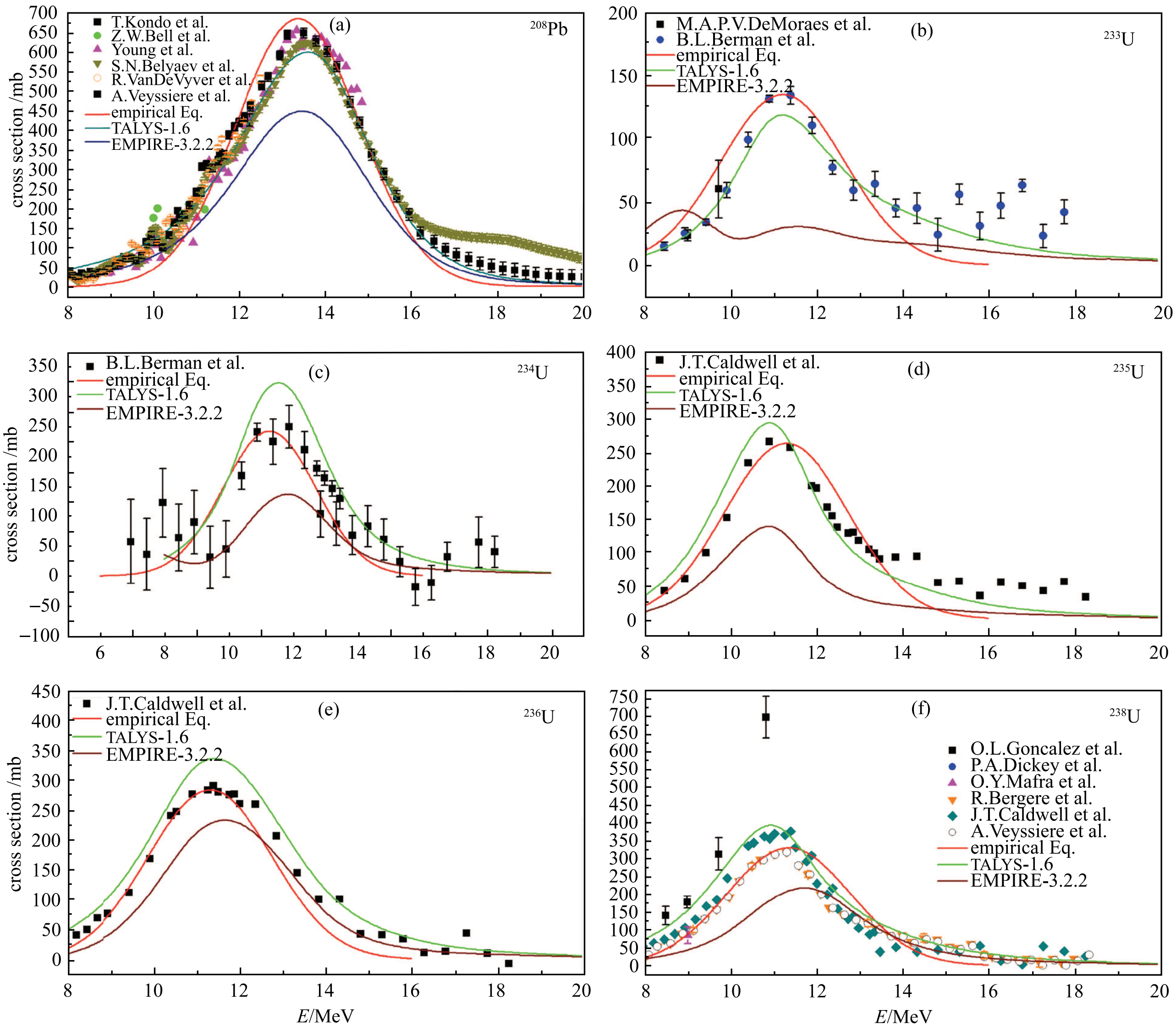

Fig. 10. (color online) Comparison of evaluated data using TALYS-1.6, EMPIRE-3.2.2, and empirical formula with experimental data from EXFOR, for ^{208}Pb, ^{233}U, ^{234}U, ^{235}U, ^{236}U, and ^{238}U.

$$S_{\rm f1}=1.39\times S_{\rm f}, \tag{17}$$

$$S_{\rm f2}=0.28\times S_{\rm f1}. \tag{18}$$

The two curves intersect at a deep point, where both curves should have the same value of cross section. This intersection point energy can be calculated by comparing the right-hand side of Eq. (12) for the above values.

$$\begin{aligned}&\sigma_{\rm m}\cdot {\rm e}^{-\frac{33.5(N-Z)}{A}}\cdot {\rm e}^{-\left(\frac{\left(Ei-S_j\cdot R_{\rm p1}\right)}{2}\right)^2}\cdot {\rm e}^{\sqrt{1+E^{\frac{2}{3}}}}\cdot S_{\rm f1}\\ =\;&\sigma_{\rm m}\cdot {\rm e}^{-\frac{33.5(N-Z)}{A}}\cdot {\rm e}^{-\left(\frac{\left(Ei-S_j\cdot R_{\rm p2}\right)}{2}\right)^2}\cdot {\rm e}^{\sqrt{1+E^{\frac{2}{3}}}}\cdot S_{\rm f2}.\end{aligned} \tag{19}$$

Solving this equation, we get

$$E_{\rm deep}=\frac{1}{2}S_j\cdot(R_{\rm p1}+R_{\rm p2})+\frac{2\ln\left(\dfrac{S_{\rm f2}}{S_{\rm f1}}\right)}{Sj\left(R_{\rm p1}-R_{\rm p2}\right)}. \tag{20}$$

This energy $E_{\rm deep}$ is near the threshold energy of the (γ, 2n) reaction. With this consideration the results are plotted in Fig. 11(a–f).

5 Applications

The (γ, n) cross section for several isotopes of W, Pb, Pa, U and Pu, which have no available experimental data, are calculated and presented using TALYS – 1.6, EMPIRE – 3.2.2 and the present empirical formula. Further, the predicted data of the isotopes were compared with different standard evaluated data libraries, wherever available.

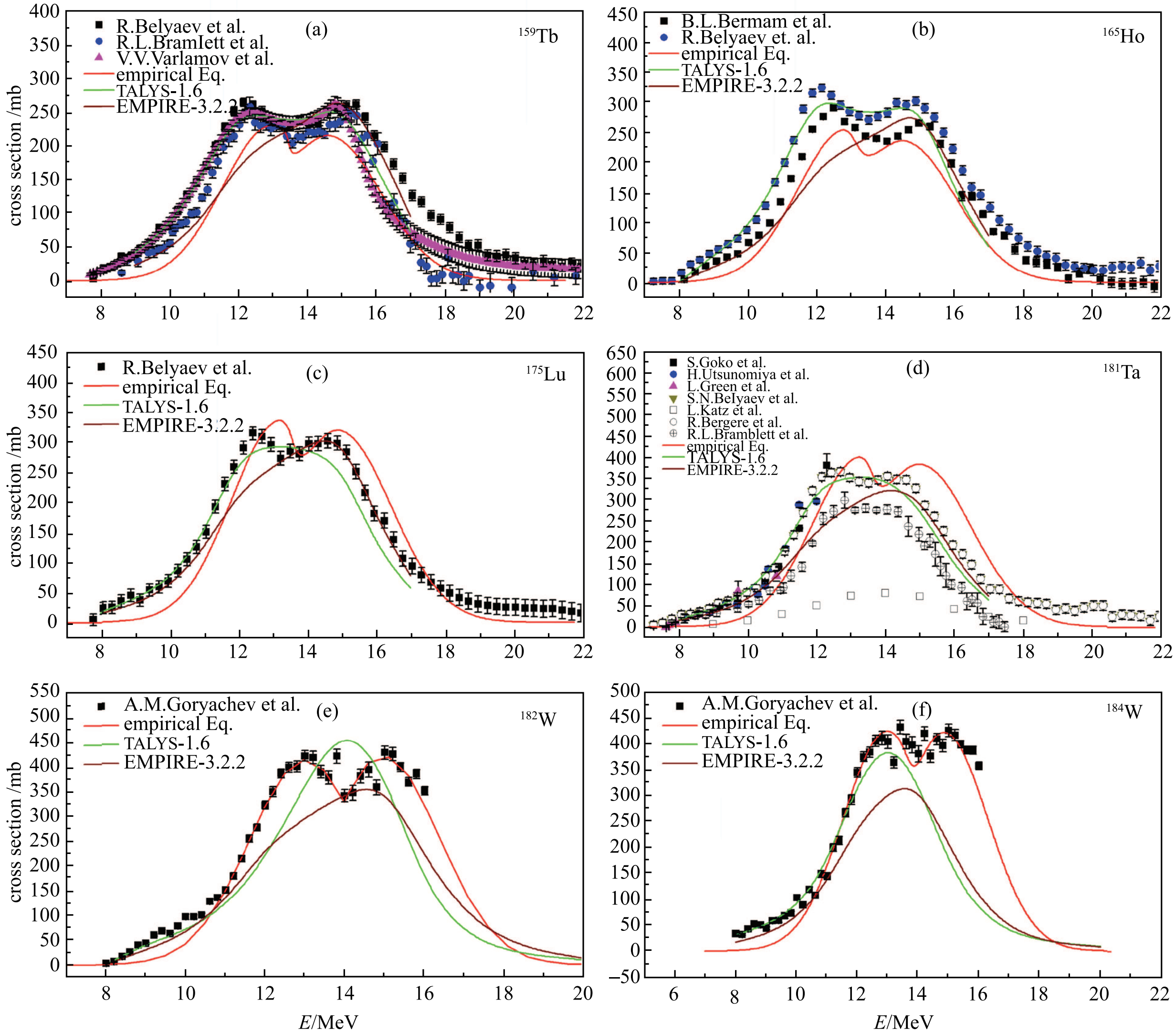

Fig. 11. (color online) Effect of deformed nuclei in (γ, n) nuclear reaction, data comparisons for TALYS – 1.6, EMPIRE – 3.2.2 and present empirical formula.

Tungsten is a prime candidate for the plasma facing component in a fusion reactor. It is selected for the diverter material in the ITER fusion reactor [4]. Tungsten isotopes ^{182}W, ^{184}W and ^{186}W have available experimental data for the (γ, n) reaction cross section [28]. The (γ, n) cross section for the remaining isotopes ^{180}W(0.12%) and ^{183}W(14.31%) are calculated and compared with the evaluated data available in ENDF/B-VII.1. No other standard data library has photonuclear data for these tungsten isotopes [18]. There is an agreement between the present evaluated data and ENDF/B-VII.1, as can be seen in Fig. 12 (a – b) data. Lead is a prime element of the Pb-Li blanket module of fusion reactors, as well as a candidate for the ADS target material [29]. Lead isotopes ^{206}Pb, ^{207}Pb and ^{208}Pb have available experimental data. The (γ, n) cross section for the remaining isotopes of lead ^{202}Pb (5.25×10^4 y, [30]), ^{203}Pb (51.92 h, [30]), ^{204}Pb (1.4×10^{17} y, [30]) and ^{205}Pb (1.73×10^7 y, [30]) are calculated and presented. These isotopes of lead have large half-lives and they face high energy photons during the runaway electron generation and the disruption phase in plasma [5]. Some isotopes of Pa and U, ^{231}Pa(3.27×10^4 y, [30]), ^{232}U(68.9 y, [30]) and ^{237}U(6.75 d, [30]), with no evaluated cross section data available in different standard data libraries such as ENDF/B-VII.1, JENDL-4.0, JEFF-3.1, ROSFOND and CENDL-3.1 [31, 32], are also calculated and presented here. The evaluated data for ^{239}Pu(2.41×10^4 y, [30]) and available data in ENDFB/VII.1 are presented in Fig. 13(d). Though in present context, the cross sections are evaluated for limited isotopes, it can be applied to calculate (γ, n) reaction cross sections for actinides using the nuclear modular codes and present empirical formula. Further, the TALYS – 1.6 and EMPIRE – 3.2.2 codes can be used to calculate the (γ, n) reaction cross section for isotopes which have available GDR parameters, whereas the present empirical formula can be used to calculate cross section for any isotope with $Z \geqslant 60$.

Another important application is that, by using the nuclear modular codes and the present formula, it is possible to calculate the incident gamma energy for which the cross section will have its maximum value, i.e. the GDR peak energy. It can be used to calculate the incident charged particle (e.g. electron) beam energy for bremsstrahlung production, which is required to design a photo neutron source. There are some theoretical transport codes available to for electrons and photons, such as MCNP [12, 33, 34], FLUKA [35, 36], GEANT [37] etc. With these codes, one can estimate the bremsstrahlung spectra from the electron beam.

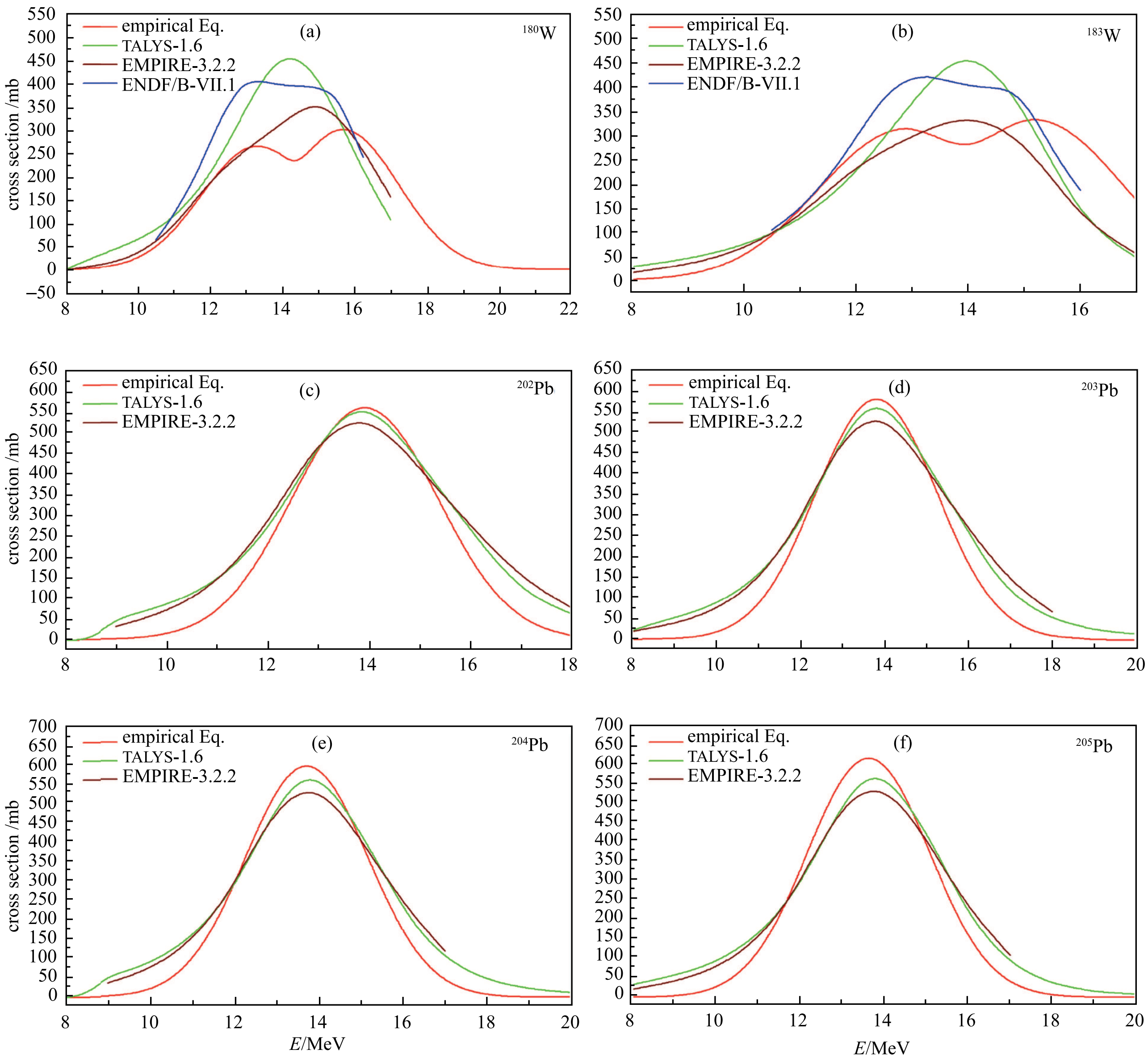

Fig. 12. (color online) Comparison of evaluated data for ^{180}W, ^{183}W, ^{202}Pb, ^{203}Pb, ^{204}Pb, ^{205}Pb using TALYS-1.6, EMPIRE-3.2.2, and empirical formula.

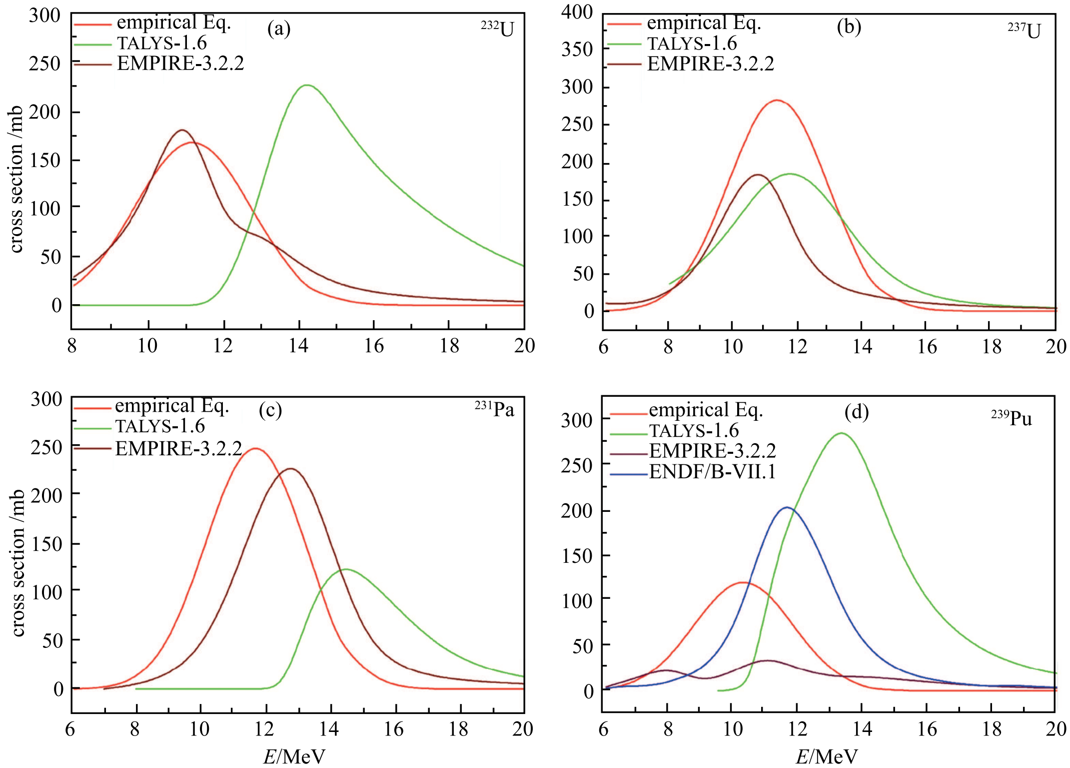

Fig. 13. (color online) Comparison of evaluated data for ^{231}Pa, ^{232}U, ^{237}U, ^{239}Pu using TALYS-1.6, EMPIRE-3.2.2, and empirical formula.

6 Conclusion

In the present work, a new empirical formula has been developed to investigate the (γ, n) reaction cross section for different isotopes with $Z \geqslant 60$ in the GDR energy region. The results for the (γ, n) reaction cross section obtained by using the above empirical formula have been reproduced by using the nuclear modular codes TALYS – 1.6 and EMPIRE – 3.2.2. It has been shown that TALYS – 1.6, EMPIRE – 3.2.2 and our empirical formula are in agreement with the experimental data. Further a conclusion may be drawn that there may be no deformation in the GDR peak of a pure (γ, n) reaction cross section for spherical nuclei. As a result of the quadrupole, which is due to the asymmetric shape of the nucleus, the present deformation has been observed.

In addition to this, the evaluated data for ^{180}W, ^{183}W, ^{202}Pb, ^{203}Pb, ^{204}Pb, ^{205}Pb, ^{231}Pa, ^{232}U, ^{237}U and ^{239}Pu using TALYS – 1.6, EMPIRE – 3.2.2 and our empirical formula have been presented. Among these only ^{180}W, ^{183}W and ^{239}Pu have evaluated data in ENDF/B-VII.1 [29], which are compared with the present evaluated data. For ^{180}W and ^{183}W, the present evaluated data are in good agreement, but in the case of ^{239}Pu, it is in disagreement. It is necessary to do experiments in the GDR energy range to validate the present evaluated data for ^{239}Pu. Further, though here only limited isotopes have been used for the (γ, n) reaction cross section evaluation, the empirical formula used in this paper may be useful for other isotopes provided $Z \geqslant 60$.

Intensive discussions with M. Herman (NNDC, Brookhaven National Laboratory, USA), R. Kapote (NAPC-Nucear Data Section, IAEA, Austria), P. K. Mehta (The M. S. University of Baroda, Vadodara), P. Mishra (The M. S. University of Baroda, Vadodara), and N. Agrawal (The M. S. University of Baroda, Vadodara) are gratefully to acknowledged.

References

1 http://www-pub.iaea.org/MTCD/publications/PDF/te_1178_prn.pdf, retrieved 16th May 2016
2 A. R. Junghans et al, Phys. Lett. B, **670**: 200 (2008)
3 S. J. Zweben, H. Knoepfel, Phys. Rev. Lett., **35**: 1340 (1975)
4 R. A. Pitts et al, Journal of Nuclear Materials, **463**: 39–48 (2013)
5 A. Shevelev et al, doi: 10.1063/1.4894038, retrieved 17th May 2016

6 B. L. Berman et al, Phys. Rev., **162**: 1098 (1967)
7 C. H. M. Broeders et al, Nucl. Eng. Des., **202**: 157 (2000)
8 F. R. Allum et al, Nucl. Phys. A, **53** 645 (1964)
9 H. Naik et al, Nucl. Phys. A, **916**: 168–182 (2013)
10 I. Raškinyteẏ et al, in Proc. Int. Conf. on Nuclear Reaction Mechanisms, (Varenna, Italy: Dapnia/SPhN, 2006), DAPNIA-06-147
11 G. Kim et al, Nucl. Instrum. Methods Phys. Res., Sect. A, **485**: 458–467 (2002)
12 V. C. Petwal et al, PRAMANA — journal of physics, **68**: 235 (2007)
13 M. Gallardo et al, Phys. Lett. B, **191**: 222–226 (1987)
14 M. Mattiuzzi et al, Phys. Lett. B, **364**: 13–18 (1995)
15 P. Heckman et al, Phys. Lett. B, **555**: 43 (2003)
16 Balaram Dey et al, Phys. Lett. B, **731**: 92–96 (2014)
17 H. Steinwedel et al, Z. Naturforsch., **5a**: 413 (1950)
18 B. L. Berman, At. Data Nucl. Data Tables, **15**: 319–390 (1975)
19 G. Reffo, Phys. Rev. C, **44**, 814 (1991)
20 S. Levinger, Phys. Rev., **84**: 43 (1951)
21 J. S. Levinger, in Nuclear Photo Disintegration (Oxford University Press, Oxford, 1960) p.54
22 A. Koning et al, TALYS – 1.6 A nuclear reaction program, (2013) p.62
23 M. Herman et al, EMPIRE – 3.2 Malta modular system for nuclear reaction calculations and nuclear data evaluation, (2013) p.18–20
24 M. Danos, Nucl. Phys., **5**: 23 (1958)
25 T. Belgya et al, Handbook For Calculations of Nuclear Reaction Data, (IAEA, Vienna, RIPL-2,IAEA-TECDOC-1506, 2006), http://www-nds.iaea.org/RIPL-2
26 V.N. Levkovski, J. Phys., **18**: 361 (1974)
27 J. S. Wang et al, Eur. Phys. J. A, **7**: 355–360 (2000)
28 https://www-nds.iaea.org/exfor/exfor.htm, retrieved $4^{\rm th}$ December 2015
29 Akito Takahashi et al, Fusion Engineering and Design, **9**: 323 (1989)
30 http://www.nndc.bnl.gov/chart/chartNuc.jsp, retrieved 2^{nd} November 2015
31 https://www-nds.iaea.org/photonuclear/, retrieved $4^{\rm th}$ December 2015
32 http://www.nndc.bnl.gov/sigma/index.jsp?dontshow=nn.6&as=9&lib=jendl3.3&nsub=20040, retrieved $4^{\rm th}$ December 2015
33 Grady Hughes, Progress in Nuclear Science and Technology, **4**: 454–458 (2014)
34 X-5 Monte Carlo Team, MCNP-A General Monte Carlo N-Particle Transport Code, Version 5, (2000) 1
35 A. Fassò et al, Advanced Monte Carlo for Radiation Physics, Particle Transport Simulation and Applications, in Proceedings of the Monte Carlo 2000 Conference, edited by A. Kling et al., (Lisbon, 2000) 159–164
36 P. K. Sahani et al, Indian J. Pure Appl. Phys, **50**: 863–866 (2012)
37 Boubaker Askri, Nucl. Instrum. Methods Phys. Res., Sect. B, **360**: 1–8 (2015)